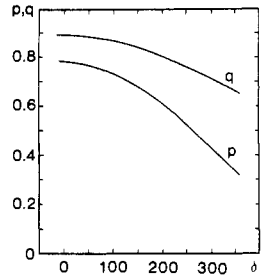

Figure 9. Calculated reduction factors p and q for the $^2E_{2g}$ ground state of the orbital doublet with linear Jahn–Teller coupling, as a function of δ with $q = {}^1/_2(1 + p)$, $\zeta = 330$ cm^{-1}, and $\Delta E(E_{2g}–E_{2g}^*) = 515$ cm^{-1}.

we can calculate p and q as a function of δ (Figure 9). In any case both p and q are significantly higher than in the case of cobaltocene, in agreement with the expectation of a weaker Jahn–Teller coupling in d^5 systems than in d^7 metallocenes.[5,6]

The INS spectrum of $Fe(C_5H_5)_2PF_6$ shows no additional peak between 200 and 400 cm^{-1} which could be assigned to a transition from the ground Kramers doublet ($^2E_{2g}$) to the suggested $^2A_{1g}$ level. The intensity ratio of the INS transitions $^2E_{2g} \rightarrow {}^2E_{2g}^*$ and $^2E_{2g} \rightarrow {}^2A_{1g}$ have been estimated for two limiting cases in the LCAO basis (eq 1) with neglect of the spreading of the spin density onto the ligands ($c_1 = c_2 = c_3 = 1$), the admixture of ligand functions ($c_1' = c_2' = c_3' = 0$), and contributions of the $^2A_{1g}$ state into the ground state.[28] Assuming axial symmetry ($\zeta \neq 0$, $\delta = 0$), the $^2E_{2g} \rightarrow {}^2A_{1g}$ transition is forbidden whereas $^2E_{2g} \rightarrow {}^2E_{2g}^*$ is allowed. If $\delta >> \zeta$, the transition $^2E_{2g} \rightarrow {}^2A_{1g}$ is theoretically half as intense as the $^2E_{2g} \rightarrow {}^2E_{2g}^*$ transition. The intensity ratio of the $Fe(C_5H_5)_2^+$ ion will be still smaller since this d^5 metallocene is situated between the two limiting cases. These results suggest that it would be difficult to locate the $^2A_{1g}$ state by INS. It is hoped that interpretation of the Raman and susceptibility data using an adequate model confirms these conclusions.

Acknowledgment. This work was supported by the Swiss National Science Foundation (Grant No. 2.442.-0.82).

Registry No. $Fe(C_5H_5)_2PF_6$, 11077-24-0; $Fe(C_5D_5)_2PF_6$, 91760-21-3; $Fe(C_5D_5)_2AsF_6$, 91760-22-4; $Fe(C_5H_5)_2I_3$, 1291-35-6; $Fe(C_5D_5)_2I_3$, 91760-23-5; $Fe(C_5H_5)_2BF_4$, 1282-37-7; $Fe(C_5H_5)_2$, 102-54-5; $Fe(C_5D_5)_2$, 12082-87-0; $Co(C_5H_5)_2$, 1277-43-6; $Co(C_5D_5)_2$, 68011-62-1; $Ni(C_5H_5)_2$, 1271-28-9; $Ni(C_5D_5)_2$, 51510-35-1; $Fe(C_5H_5)_2^+$, 12125-80-3; $Co(C_5H_5)_2^+$, 12241-42-8.

Contribution from the Department of Chemistry and Chemical Physics Program, Washington State University, Pullman, Washington 99164-4630

Forbidden Vibrational Modes in Iron(II), Ruthenium(II), and Osmium(II) Hexacyanides: A Tunneling, IR, and Raman Spectroscopy Study

K. W. HIPPS,* STEPHEN D. WILLIAMS, and URSULA MAZUR

Received December 20, 1983

Two of the optically forbidden vibrational fundamentals of the iron-group hexacyanides were directly observed by inelastic electron tunneling spectroscopy. Assignments for these modes in the case of iron(II) hexacyanide are based on their positions, isotopic shifts, and agreement in position of observed bands with those calculated by using an extensively applied valence force potential. Assignments of the optically forbidden modes in the cases of ruthenium and osmium are made by comparing IETS positions and intensities with those observed in the case of iron. Our results support and extend much of the previous work on hexacyanides of the iron-group metals. Some of our assignments for osmium(II) and ruthenium(II) hexacyanides, based on tunneling and polarized Raman data, differ from those previously suggested. One important aspect of this paper is the general observation that tunneling spectroscopy can be used to provide information that is not directly available from Raman and IR studies. Further, IETS lines are somewhat narrower than solution-phase Raman lines. Thus, tunneling spectroscopy is an important new technique complementary to Raman and IR spectroscopy.

Introduction

Understanding the forces that produce molecules from atoms is one of the primary goals of modern inorganic chemistry. These forces are most commonly and easily studied by vibrational spectroscopy. The observed frequencies of fundamental vibrations can be directly related to the forces that hold the molecule together near its equilibrium geometry. Analysis of overtone and combination bands can extend this information to regions somewhat distant from the equilibrium configuration. The analysis of these vibrational data yields force constants that are determined by, and provide information about, the electronic structure of molecules. The methods by which this analysis is performed are well-known and have been extensively applied in inorganic chemistry.[1–4] The primary experimental tools, to date, have been IR and Raman spectroscopy.

While IR and Raman methods have provided a rich yield of information about forces in inorganic systems, they are intrinsically limited by the selection rules that govern the absorption and scattering of light. For example, of the 13 fundamental frequencies of a metal hexacyanide ion, 6 are Raman active, 4 are IR active, and 3 are inactive in both IR and Raman. Thus, a significant portion of the ion's spectrum and the corresponding information about molecular forces are not directly available to the optical spectroscopist. Further, this situation is not unique to the case of octahedral ions. Even for systems of relatively low symmetry (such as C_{3v}), optically inactive bands occur. While these forbidden bands may be observed as combinations or overtones and have frequently been assigned in this manner, these assignments are often ambiguous.

A new vibrational spectroscopy, complementary to IR and Raman but governed by different selection rules, is clearly

* To whom correspondence should be addressed at the Department of Chemistry.

(1) Jones, L. H. "Inorganic Vibrational Spectroscopy"; Marcel Dekker: New York, 1971; Vol. 1.
(2) Adams, D. M. "Metal-Ligand and Related Vibrations"; Edward Arnold: London, 1967.
(3) Nakamoto, K. "Infrared and Raman Spectra of Inorganic and Coordination Compounds", 3rd ed.; Wiley: New York, 1978.
(4) Wilson, E. B.; Decius, J. C.; Cross, P. C. "Molecular Vibrations"; Dover Publications: New York, 1955.

0020-1669/84/1323-3500$01.50/0

needed to further our knowledge about molecular force fields. We believe that inelastic electron tunneling spectroscopy (IETS) is the required technique. Theoretical[5] and experimental[6-11] evidence has indicated that the selection rules operative in IETS are very different from those that apply to optical spectroscopy. In fact, there is experimental evidence that IR- and Raman-inactive transitions can be observed by IETS.[8-11] Further, the utility of IETS for the study of inorganic species has been demonstrated with a variety of compounds, ions, and metal complexes.[9-13] While there are experimental limitations on what type of system can be studied by IETS,[11] tunneling can be used to study many broad classes of materials.

The purpose of the present paper is threefold. First, we will thoroughly document the observation by IETS of two of the three forbidden modes in three iron-group hexacyanides. Second, we will utilize these observations to determine force constants for the ferrocyanide ion. And third, we will provide correct assignments for most of the vibrational modes of the divalent iron-group hexacyanide. Overshadowing these particular goals is our desire to demonstrate in an unequivocal manner that tunneling spectroscopy is a mature technique of real value to the vibrational spectroscopist.

Experimental Section

Materials. $K_4Fe(CN)_6 \cdot 3H_2O$ and $K_4Ru(CN)_6 \cdot 3H_2O$ were obtained commercially and recrystallized from water before use. $K_4Os(CN)_6 \cdot 3H_2O$ obtained from several commercial sources was of unsatisfactory quality. The osmium(II) hexacyanide used in this study was prepared by the method of Krauss and Schrader[14] and recrystallized twice from water. Isotopic iron(II) hexacyanides were prepared by methods previously described.[9] All metal cyanide solid spectra were taken from powdered samples. Aluminum and lead metals used to form tunnel junctions were 99.999% pure.

It is important to note that the trihydrates rapidly dehydrate when exposed to low-humidity atmospheres or more than about 50 mW of 5145-Å laser radiation. The final hydration number of the material depends on its history. $K_4Fe(CN)_6 \cdot xH_2O$, for example, forms with $x = {}^1/_2$ after about 10 h of storage in a vacuum desiccator. The spectra of the partially hydrated hexacyanides differ from those of the trihydrates; some of these differences will be displayed and utilized in later sections. In general, when we refer to partially hydrated material, x will be ill-defined and less than 1. Trihydrate spectra were obtained from complexes that were recrystallized from water immediately before use, ground to powder, sealed in a capillary tube, and then exposed to no more than 15 mW of 5145-Å radiation. Sufficient ferrocyanide was available to allow an additional experiment to be performed. Freshly recrystallized potassium ferrocyanide was ground with water to form a thick slurry. This slurry was sealed in a 5-mm NMR tube, and the Raman spectrum was measured with 5 mW of 5145-Å laser power. The spectrum obtained from this sample was identical with those obtained from trihydrate powders.

Raman Spectroscopy. Raman spectra were measured with a double 1-m ISA Ramanor spectrometer having a dispersion of 2.5 Å/mm, a Spex DPC2 photon counter, and either a Lexel Kr ion or Spectra-Physics Ar ion laser. The spectrometer and photon counter were controlled by a Cromenco computer, and most of the spectra represent the sum of many repeated scans. The polarization of the incident laser radiation was controlled by a polarization rotator, and scattered radiation was passed through a polarization scrambler. Solid samples were studied as powders, and polarized aqueous solution measurements were made either in a rectangular quartz cell or, in the case of osmium(II) hexacyanide, in a capillary tube. A 90° scattering geometry was used throughout. Slit widths of 0.3 and 1.0 mm were typical for solid and solution samples, respectively.

The symmetric and asymmetric parts of the solution-phase Raman spectra were obtained in the following manner. Consider the sample solution located at the origin of coordinates with the laser located at $+y$ and the entrance slits of the monochromator located at $+x$. When the laser is polarized along z, the intensity observed is designated I_z. Polarization of the laser radiation along x yields intensity I_x. The intensity I_x as a function of energy is the asymmetric part, I_a, of the Raman spectrum. The symmetric part, I_s, is defined as $I_z - (7I_x/6)$.

IR Spectroscopy. Infrared spectra were measured on a Perkin-Elmer 283B instrument. Samples were run either as KBr wafers or as petroleum jelly mulls. Typical instrumental resolution was <3 cm^{-1}. Polystyrene was used to calibrate the cm^{-1} axis of the spectrometer.

IETS. All of the tunnel junctions used in this study were of the form $Al-Al_2O_3-M(CN)_6^{4-}-Pb$. The hexacyanide ion was incorporated in the junction by aqueous solution-phase adsorption on the aluminum oxide. Typical solution concentrations were about 0.5 mg/mL. The method of junction fabrication and a detailed description of the spectrometer used here was given by Hipps and Mazur.[10] High-resolution tunneling spectra were measured below 1.8 K with less than 0.7 mV rms modulation amplitude. In some cases the reported spectra are the sum of several repeated scans.

In order to obtain tunneling spectra in the 100–300-cm^{-1} range, a few of the tunnel diodes were placed between a pair of Sm–Co permanent magnets. These magnets were sufficiently strong to quench the superconductivity of the lead top electrode and, therefore, to eliminate the intense lead superconducting phonon structure in this region.

It should be noted that the local environment in the tunnel junction is not the same as either crystalline or aqueous samples. There is, however, a marked cation dependence in band positions observed by IETS for the H^+ through Cs^+ salts of ferrocyanide.[10] Thus, the cations are in near-proximity to the complex ion.

Methods

The force field calculation described in this paper was performed by utilizing a force field first proposed by Jones[15] and later applied to iridium(III), rhodium(III), and cobalt(III) hexacyanides.[16] The **F** and **G** matrices given by Jones[15] were used to obtain the vibrational energies from a given set of force constants. The method of force constant optimization, however, was somewhat nonstandard and is described in detail in an earlier publication.[17] Briefly, the array of all force constants is required to give a minimum error for all weighted bands; i.e.

$$\sum(\nu_i^{\text{calcd}} - \nu_i^{\text{exptl}})^2 = \text{minimum}$$

Thus, all modes that are affected by a given force constant contribute toward the determination of that force constant.[17] This is an unconventional approach in that frequency errors, rather than eigenvalue errors, are minimized. For the ferrocyanide fit reported here, 30 frequencies were simultaneously fit by a 10-parameter potential function. All of the 30 observed frequencies were equally weighted. In this procedure, a weight of 1.0 for all fitted bands is equivalent to the assumption of equal frequency accuracy for each band. Errors in low- and high-frequency bands are equally significant.

Results

Figure 1 contrasts the medium-resolution tunneling and Raman spectra obtained from the $Ru(CN)_6^{4-}$ ion. $K_4Ru(CN)_6 \cdot 3H_2O$ was used to provide the Raman spectrum. On this scale, the spectra of all three metal cyanides are similar. For future reference, it is important to note that the tunneling intensities are distributed very differently than are the Raman intensities. The metal–cyanide bending bands (below 700 cm^{-1}) are the dominant feature in the tunneling spectrum. The CN stretches (near 2000 cm^{-1}) and the lattice motions (below 200 cm^{-1}) dominate the Raman spectrum. Except for the lack

(5) Kirtley, J. In "Tunneling Spectroscopy"; Hansma, P. K., Ed.; Plenum Press: New York, 1982; Chapter 2.
(6) de Cheveigne, S.; Klein, J.; Leger, A. In "Tunneling Spectroscopy"; Hansma, P. K., Ed.; Plenum Press: New York, 1982; Chapter 4.
(7) Hipps, K. W.; Keder, J. W. *J. Phys. Chem.* **1983**, *87*, 3186.
(8) Kirtley, J.; Hansma, P. K. *Surf. Sci.* **1977**, *66*, 125.
(9) Hipps, K. W.; Mazur, U.; Pearce, M. S. *Chem. Phys. Lett.* **1979**, *68*, 433.
(10) Hipps, K. W.; Mazur, U. *J. Phys. Chem.* **1980**, *84*, 3162.
(11) Hipps, K. W.; Mazur, U. In "Tunneling Spectroscopy"; Hansma, P. K., Ed.; Plenum Press: New York, 1982; Chapter 8.
(12) Weinberg, H. W. In "Tunneling Spectroscopy"; Hansma, P. K., Ed.; Plenum Press: New York, 1982; Chapter 12.
(13) Hipps, K. W. *J. Electron Spectrosc. Relat. Phenom.* **1983**, *30*, 275.
(14) Krauss, F.; Schrader, G. *J. Prakt. Chem.* **1929**, *119*, 279.
(15) Jones, L. H. *J. Mol. Spectrosc.* **1962**, *8*, 105.
(16) Jones, L. H. *J. Chem. Phys.* **1964**, *41*, 856.
(17) Hipps, K. W.; Poshusta, R. D. *J. Phys. Chem.* **1982**, *86*, 4112.

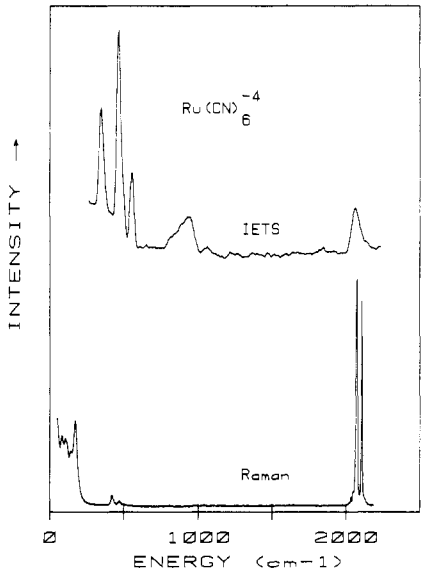

Figure 1. Medium-resolution inelastic electron tunneling and Raman spectra of ruthenium(II) hexacyanide. The Raman spectrum was obtained from solid $K_4Ru(CN)_6 \cdot 3H_2O$.

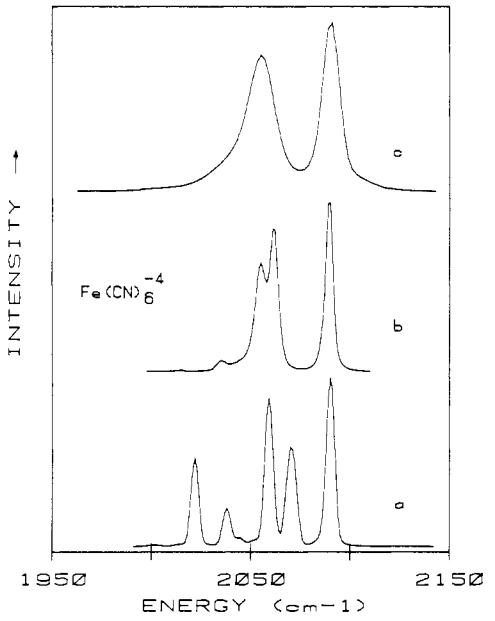

Figure 2. Raman spectra of ferrocyanide in the CN-stretching region: (a) solid potassium ferrocyanide x-hydrate; (b) solid potassium ferrocyanide trihydrate; (c) aqueous potassium ferrocyanide.

of lattice motions, this is also true in the case of solution-phase Raman spectra. The very broad band near 980 cm^{-1} in the tunneling spectrum is due to the Al–O stretching motion of the oxide support. No strong bands occur in the tunneling spectrum between 100 and 300 cm^{-1}.

Figure 2 shows the aqueous (part c) and solid (part b) potassium ferrocyanide trihydrate and solid potassium ferrocyanide x-hydrate (part a) Raman spectra in the CN-stretching region. The band at 2055 cm^{-1} in Figure 2c is partially resolved into two bands centered at 2059 cm^{-1} in Figure 2b. The band near 2090 cm^{-1} in the solution spectrum is polarized while the 2055-cm^{-1} band is not. Thus we assign them to the a_{1g} and e_g stretches, respectively. In the x-hydrate spectrum (Figure 2a), the site symmetry is so low that the e_g and t_{1u} modes are considerably split and some t_{1u} intensity is seen in the Raman. The band shapes shown in Figure 2 for ferrocyanide ion are quite similar to those obtained for the ruthenium and osmium cyanides. The peak positions, of course, vary with metal ion. The e_g frequencies for the trihydrate salts given later were chosen as the center of the doublet in the solid-state Raman spectra.

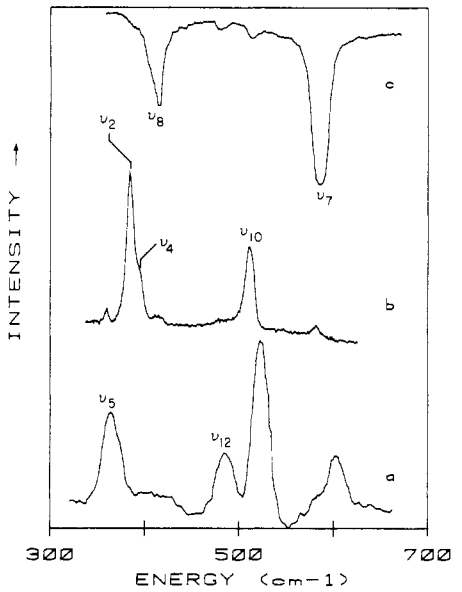

Figure 3. Vibrational spectra obtained from the ferrocyanide ion: (a) IETS; (b) solid-state Raman spectrum of potassium ferrocyanide trihydrate; (c) IR spectrum of potassium ferrocyanide trihydrate in KBr.

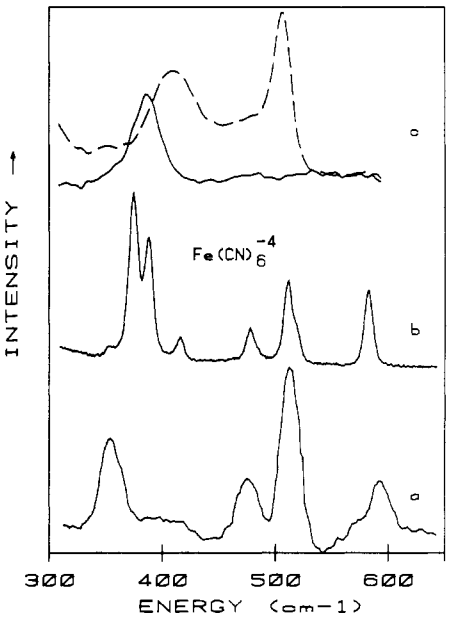

Figure 4. Vibrational spectra of the ferrocyanide ion obtained with three different techniques: (a) tunneling spectrum; (b) solid-state Raman spectrum of potassium ferrocyanide x-hydrate; (c) symmetric (solid line) and asymmetric (broken line) parts of the aqueous-solution Raman spectrum.

Figure 3 presents the inelastic electron tunneling (IET) spectrum of the ferrocyanide ion (part a) and also the Raman (part b) and IR (part c) spectra of $K_4Fe(CN)_6 \cdot 3H_2O$ in the 300–700-cm^{-1} region. Note that while the solid-state Raman spectrum has somewhat narrower lines, the line widths observed in all three types of spectra are similar. Figure 4 contrasts the tunneling (part a) and aqueous polarized Raman spectra (part c) of the ferrocyanide ion with the solid-state Raman spectrum obtained from the x-hydrate material (part b). Comparison of Figure 4b with Figure 3b shows that dehydrating the solid has relatively little effect on the positions of bands; the largest shift is in ν_2, which moves down by about 9 cm^{-1}. The dramatic effect of dehydration is to disrupt the

Table I. Observed and Calculated Positions of Vibrational Fundamentals for Potassium Ferrocyanide Trihydrate Based on a Ten-Parameter Potential

mode		ν_{obsd}, cm^{-1}	ν_{calcd}, cm^{-1}	$\Delta(^{13}C)$ obsd	$\Delta(^{13}C)$ calcd	$\Delta(^{15}N)$ obsd	$\Delta(^{15}N)$ calcd	ref
a_{1g}	ν_1	2090	2088	−45	−47	−29	−30	*b*
	ν_2	385	386	−7	−7	−7	−8	*b*
e_g	ν_3	2059	2055	−44	−47	−29	−29	*b*
	ν_4	392	393	−8	−7	−8	−8	*b*
t_{1g}	ν_5	354	355	−9	−10	−1	−3	*d*
t_{1u}	ν_6	2044	2049	−47	−45	−35	−30	*c*
	ν_7	586	588	−11	−13	−1	−3	*c*
	ν_8	415	413	−7	−6	−6	−5	*c*
	ν_9	...	83	...	−1	...	−2	
t_{2g}	ν_{10}	511	511	−18	−17	−1	−2	*b*
	ν_{11}	...	113	...	−1	...	−3	
t_{2u}	ν_{12}	474	475	−16	−15	0	−3	*d*
	ν_{13}	...	61	...	−1	...	−2	

σ = 3.2 cm^{-1}; mean percentage error 0.25%

[a] $\Delta(^{13}C) = \nu(^{13}C) - \nu(^{12}C)$ and $\Delta(^{15}N) = \nu(^{15}N) - \nu(^{14}N)$. [b] Trihydrate Raman data. [c] Trihydrate IR data (in KBr). [d] Tunneling data.

Table II. Observed Fundamentals (cm^{-1}) and Assignments for Iron, Ruthenium, and Osmium Hexacyanide Ions[a]

mode	$Fe(CN)_6^{4-}$	$Ru(CN)_6^{4-}$	$Os(CN)_6^{4-}$	source
ν_1	2090	2108	2109	aq Raman
ν_2	385[c]	425	458	
ν_3	2055	2068	2061	
ν_4	409[c]	425	449	
ν_5	354	344	362[d]	IETS
ν_6	2044	2048	2038	IR (KBr)
ν_7	586	550	555	
ν_8	415	371	(390)	
ν_9				
ν_{10}	506	465	476[b]	aq Raman
ν_{11}	(105)			
ν_{12}	474[d]	491[b]	513[d]	IETS
ν_{13}				

[a] Values in parentheses are taken from ref 18. [b] Values differ significantly from those given in ref 18. [c] The order of these values is reversed in ref 18 but similar to the order given in ref 19. [d] No value previously available.

site symmetry to the extent that several new bands appear. Two of these are clearly the IR-active modes ν_7 and ν_8. The third, near 475 cm^{-1}, is at the same position as one of the bands seen in the tunneling spectrum.

Table I contains the peak positions observed for several isotopic forms of the ferrocyanide ion. In cases where bands are observed by more than one technique (e.g., ν_7 can be extracted from the IR, tunneling, or *x*-hydrate Raman data), the spectroscopy in which the band is formally allowed and for which trihydrate data were available was chosen. Thus, the frequencies given are the best set for analyzing potassium ferrocyanide trihydrate. Table II is a collection of the observed fundamental frequencies chosen to best represent the isolated ferrocyanide ion.

Figures 5 and 6 show the tunneling (part a), aqueous polarized Raman (part c), and trihydrate solid Raman spectra (part b) for ruthenium and osmium hexacyanide, respectively. Comparison of Figures 4c, 5c, and 6c indicates that the lower frequency depolarized band, ν_4, changes in relative position with respect to the polarized band ν_2, as one proceeds down the periodic table. This is also reflected in the solid-state data (Figure 4b, 5b, and 6b) wherein sidebands are seen to the right and left of the most prominent band in the case of iron and osmium, respectively, but no shoulder is seen in the case of ruthenium hexacyanide trihydrate. Table II collects the observed fundamentals of ruthenium and osmium hexacyanides selected from polarized aqueous Raman, IR (in KBr), and IETS data. The frequencies presented in Table II, therefore, are close approximations to those of the free ion.

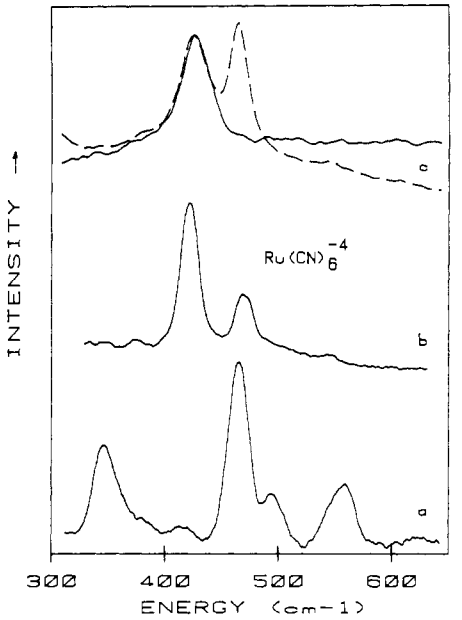

Figure 5. Vibrational spectra of the ruthenium(II) hexacyanide ion obtained with three different techniques: (a) tunneling spectrum; (b) solid-state Raman spectrum of potassium hexakis(cyanato)ruthenate(II) trihydrate; (c) symmetric (solid line) and asymmetric (broken line) part of the aqueous-solution Raman spectrum.

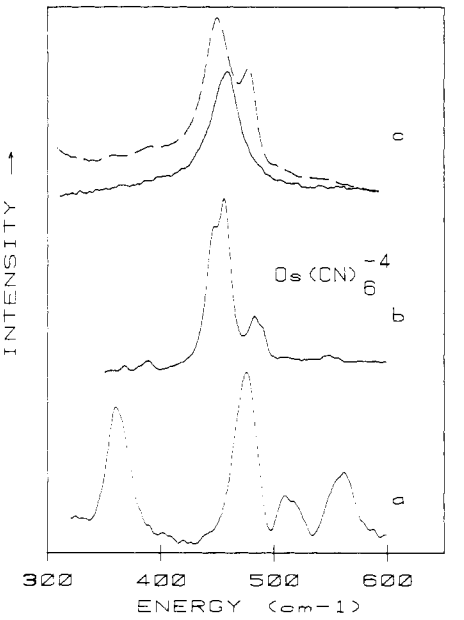

Figure 6. Vibrational spectra of the osmium(II) hexacyanide ion obtained with three different techniques: (a) tunneling spectrum; (b) solid-state Raman spectrum of potassium hexakis(cyanato)osmate(II) trihydrate; (c) symmetric (solid line) and asymmetric (broken line) parts of the aqueous-solution Raman spectrum.

Discussion

Ferrocyanide Assignments. The vibrational spectrum of the ferrocyanide ion has been discussed by many authors.[1-3,9-11,18-23] Of these, Nakagawa and Shimanouchi[21]

(18) Griffith, W. P.; Turner, G. T. *J. Chem. Soc. A* **1970**, 858.
(19) Swanson, B. I.; Rafalko, J. J. *Inorg. Chem.* **1976**, *15*, 249.
(20) Jones, L. H.; Swanson, B. I.; Kubas, G. J. *J. Chem. Phys.* **1974**, *61*, 4650.
(21) Nakagawa, I.; Shimanouchi, T. *Spectrochim. Acta* **1962**, *18*, 101.

provided the most complete force field analysis. Unfortunately, their study did not include isotopic substitution and it appears that their analysis is flawed. The most obvious problem associated with their treatment is the description of ν_7 as a stretching mode. Detailed normal-coordinate calculations[1,20] indicate that large ^{13}C shifts are characteristic of MCN-bending modes. Hence, the large ^{13}C shift observed here indicates that ν_7, not ν_8, is a bending mode. A pictorial representation of the modes of the iron-group cyanides is available on page 13 of ref 23. Swanson[19] has reported some of the isotopic bands of the ferrocyanide ion in solution, and Griffith[18] has given a relatively complete set of assignments for both the trihydrate and the anhydrous potassium salt, but without isotopic data or a force field determination. Our trihydrate assignments are more complete than and differ somewhat from those of Griffith.[18] Our solution-phase Raman data and assignment agree well with those of Swanson.[19]

The assignment of the CN-stretching motions is straightforward. The 2090-cm^{-1} band is totally polarized in the Raman spectrum and therefore corresponds to the a_{1g} stretching mode, ν_1. This band appears in essentially the same place in the trihydrate salt. The depolarized Raman solution band at 2055 cm^{-1} in solution shifts and splits somewhat in the trihydrate to form a pair of bands centered at 2059 cm^{-1}. Thus, we assign these as the e_g-symmetry CN stretch ν_3. The very strong and broad IR band centered near 2044 cm^{-1} is the t_{1u} CN stretch, ν_6.

The other Raman-active bands are assigned as follows. The depolarized solution band appearing at 506 cm^{-1} corresponds to the band at 511 cm^{-1} in the trihydrate Raman spectrum and at 511 cm^{-1} in the tunneling spectrum; all have identical isotopic shifts. The ^{13}C shift of this band is more than twice that of the other two bands observed in this region, and its ^{15}N shift is negligible. Thus, it is assigned as the t_{2g} bending band, ν_{10}. The other depolarized band in this region occurs at 409 cm^{-1} and must be the e_g mode, ν_4. The polarized solution band at 385 cm^{-1} is the a_{1g} band ν_2. In the trihydrate solid, ν_2 and ν_4 occur with almost equal energy. In the *x*-hydrate, they are again resolvable. Griffith has assigned the lower frequency solid-state band (385 cm^{-1}) as ν_4 and the higher energy one (392 cm^{-1}) as ν_2. We have chosen the opposite ordering. We do so because, in all three metal cyanides reported here, it appears that the ν_2, ν_4 ordering is preserved in going from solution to solid state (see Figures 4, 5, and 6). It is important to note, however, that the choice of ordering of these bands does not affect any of the other assignments and arguments.

We have observed two of the three IR-active metal–cyanide motions. The band at 586 cm^{-1} in the IR spectrum, and at 591 cm^{-1} in the tunneling spectrum, has a large ^{13}C isotope shift and a small ^{15}N shift. Thus, it is primarily a metal–cyanide bending motion, the t_{1u} mode ν_7. The band at 415 cm^{-1} in the IR spectrum has roughly equal ^{13}C and ^{15}N isotope shifts and is assigned as the t_{1u} stretching band, ν_8. It should be noted that these bands also appear in the Raman spectrum of potassium ferrocyanide *x*-hydrate (Figure 4b).

The only strong bands remaining to be assigned in Figures 3 and 4 occur at 354 and 474 cm^{-1} in the tunneling spectrum. The 354-cm^{-1} band is absent or very weak in all IR and Raman spectra, but the 474-cm^{-1} band appears in the *x*-hydrate Raman spectrum. Both of these bands have large ^{13}C shifts and small ^{15}N shifts, suggesting that they are primarily bending modes. The only remaining fundamentals expected to behave in this fashion with isotopic substitution are the t_{1g} mode, ν_5, and the high-frequency t_{2u} mode, ν_{12}. No possible combination bands, other than those involving ν_5 and ν_{12}, can produce the large isotopic shifts seen (see Table I). Griffith[18] suggested a value of 350 cm^{-1} for ν_5 on the basis of combination bands seen in the IR spectrum, and we assign the 354-cm^{-1} band seen in the tunneling spectrum as ν_5. The 474-cm^{-1} band is assigned as ν_{12}.

Table III. Potential Constants for d^6 Metal Hexacyanides

	$K_4Fe(CN)_6 \cdot 3H_2O$[a]	$K_3Co(CN)_6$[b]	$K_3Rh(CN)_6$[b]	$K_3Ir(CN)_6$[b]
F_{CN}	15.52	16.76	16.83	16.67
F_{MC}	1.99	2.06	2.37	2.70
F_β	0.58	0.52	0.53	0.57
F_α	0.21	0.29	0.28	0.29
$F''_{CN,CN}$	0.09	0[c]	0[c]	0[c]
$F'_{MC,MC}$	0.46	0.46	0.75	0.69
$F''_{MC,MC}$	−0.02	0.04	0.03	0.05
$F'_{\beta,\beta}$	0.11	0.08	0.05	0.04
$F''_{\beta,\beta}$	0.06	0.04	0.04	0.02
$F'''_{\beta,\beta}$	0.05	0.06	0.04	0.04

[a] This work. [b] Taken from ref 16. [c] Fixed at zero in ref 16.

With use of these assignments for 10 fundamentals of each of the $^{12}C^{14}N$, $^{13}C^{14}N$, and $^{12}C^{15}N$ isotopomers, a total of 30 frequencies were fit, by methods described in a previous section, to a 10-parameter potential proposed by Jones.[15,16] The calculated results and assignments for potassium ferrocyanide trihydrate are given in Table I. The standard deviation (3.2 cm^{-1}) and mean percentage error (0.25%) of the fit are excellent. Table III provides the values obtained for the 10 force constants used. Also shown in Table III are the results obtained by Jones for the isoelectronic cobalt(III), rhodium(III), and iridium(III) complexes.[16] Comparison of our results with those of Jones, as presented in Table III, indicates that all but one of the force constants compare well across the series. The change in sign of $F''_{MC,MC}$ is due entirely to our choice in the order of ν_2 and ν_4. In cobalt(III), rhodium(III), iridium(III), ruthenium(II), and osmium(II) hexacyanide, the energy of ν_2 equals or exceeds the energy of ν_4. In iron(II) hexacyanide ν_2 lies below ν_4. While one may argue against our ordering for the solid-state data, there is no question that ν_4 lies above ν_2 for the ferrocyanide ion in solution.

Osmium and Ruthenium Hexacyanide Assignments. Vibrational assignments for ruthenium(II) and osmium(II) hexacyanides have been proposed by several authors.[18,21,24-26] Of these, the assignments of Griffith[18] are the most complete. As we mentioned earlier, the force field calculations of Nakagawa and Shimanouchi[21] are flawed because of their assumption that the metal–cyanide t_{1u} bending mode lay below the metal–cyanide stretching mode. Further, their assignments for ν_{10} and ν_{12} are clearly in error (vide infra).

When Figures 4–6 are compared and the assignments presented in Tables I and II are used, the normal modes of the ruthenium and osmium hexacyanides can be assigned in a simple fashion. The CN-stretching modes are directly assigned by their solution-state polarization in the Raman spectra and by the location of the t_{1u} CN-stretching mode in the IR spectra. The mode near 550 cm^{-1} in the IR and tunneling spectra of both the osmium and ruthenium hexaycanides is obviously the t_{1u} bending mode, ν_7. The depolarized band near 465 and 476 cm^{-1}, in the Raman and tunneling spectra of ruthenium and osmium hexacyanides, respectively, is the t_{2g} bending mode, ν_{10}. The a_{1g} and e_g metal–cyanide stretching modes are absent in the tunneling spectra but are clearly identified in both the polarized solution Raman and the solid-state Raman spectra. The two remaining bands in the

(22) Dunsmuir, J. T.; Lane, A. P. *J. Chem. Soc. A* **1971**, 776.
(23) Sharpe, A. G. "The Chemistry of Cyano Complexes of the Transition Metals"; Academic Press: New York, 1976.
(24) Mathieu, J. P.; Poulet, H. *Spectrochim. Acta* **1964**, *19*, 1966.
(25) Mathieu, J. P.; Poulet, H. *C.R. Hebd. Seances Acad. Sci.* **1959**, *248*, 2315.
(26) Hidalgo, A.; Mathieu, J. P. *C.R. Hebd. Seances Acad. Sci.* **1959**, *249*, 233.

tunneling spectrum are assigned, in analogy with the iron results, as ν_5 and ν_{12}. Our assignments for ruthenium(II) and osmium(II) hexacyanide are also collected in Table II.

The solution and solid-state Raman data indicate that the separation between ν_2 and ν_{10} decreases with increasing atomic number. The e_g metal–cyanide band, ν_4, moves from a position of higher energy relative to ν_2, in the case of the iron complex, to near degeneracy with ν_2 in the case of ruthenium and to a position of lower energy in the case of osmium. The position of the t_{2u} bending mode ν_{12} is also quite metal dependent; it increases with frequency with increasing atomic number.

Tunneling Data. The positions of tunneling bands and their isotopic shifts are very helpful in assigning the vibrational spectra of the iron-group hexacyanides. The positions of bands observed by IR or Raman as well as by IETS agree well with each other. Isotope shifts measured by tunneling are completely consistent with those observed by other methods or calculated in the force field analysis. The line widths of tunneling bands are broader than those obtained by Raman spectroscopy of solids but are very similar to IR and solution-phase Raman bands. The values obtained for ν_5 for the iron and ruthenium complexes are very similar to those reported by Griffith[18] based on the assignment of combination bands. Of even more significance is our observation of several fundamentals that were previously unknown; these are labeled by footnote *d* in Table II. Thus, tunneling has both assisted in the assignment of bands seen in IR and/or Raman spectra and has provided information that was not available from these techniques.

We have not employed any type of selection rules for the tunneling process in our analysis of these vibrational spectra. It is both natural and appropriate to ask, "What are the selection rules for tunneling?" Unfortunately, no general answer to this question is presently available, although several groups are trying to establish selection rules.[5,8,27-29] Some general observations based on empirical data can be stated: (a) bands seen by tunneling spectroscopy are almost always fundamentals; (b) the tunneling spectrum is not simply a modified IR or Raman spectrum—its selection rules are different; (c) vibrational transitions forbidden in IR and Raman spectroscopy can be observed by IETS. Considering the results of the present study, yet another empirical observation can be added; in the case of octahedral complexes, the metal–ligand bending motions are the most intense features in the tunneling spectrum. This result is both useful and surprising. None of the existent theories of IETS can account for this observation. They all utilize an electron–dipole, electron–partial-charge, or electron–induced-dipole (Raman-like) interaction mechanism. In the case of the iron-group hexacyanides, the CN-stretching motions have both the largest induced dipole and the largest dipole derivatives of any of the normal modes. Thus, these theoretical treatments would predict that the CN-stretching band is the most intense, in contradiction to the observed intensities. In this content, it is interesting to note that the metal–cyanide bending motions in metal carbonyl tunneling spectra are also the most intense features.[30-32]

Conclusions

Tunneling, Raman, and IR spectroscopy were used to assign 10 of the 13 fundamental vibrations of several metal hexacyanide complexes of the form $M(CN)_6^{4-}$. Carbon-13, nitrogen-15, and normal isotopic data were obtained from the ferrocyanide ion, and the 30 observed frequencies were fit to a 10-parameter potential. This potential was previously employed by Jones for analyzing other isoelectronic metal hexacyanides.[15,16] The force constants obtained for the ferrocyanide ion are quite similar to those obtained by Jones for cobalt(III), rhodium(III), and iridium(III) hexacyanides. Calculated positions for all 13 fundamentals for each of the three isotopomers are given.

The positions, line widths, and isotopic shifts of bands observed by both tunneling and IR or by both tunneling and Raman spectroscopy agree within the small variations expected due to environmental effects. In addition, two fundamentals that are forbidden in IR and Raman spectroscopy were observed. Thus, tunneling spectroscopy makes a significant contribution to the identification of the normal modes of these hexacyanides. It is observed that the metal–cyanide bending motions are the most intense features in the tunneling spectrum of the M(II) hexacyanides studied here. Carbon–nitrogen stretching motions are weak and unresolved but easily observed. This lack of resolution may be due to image–dipole interactions with the top metal.[33] Metal–cyanide stretching motions are very weak or absent in the tunneling spectrum.

Acknowledgment. This material is based upon work supported by the National Science Foundation under Grant No. DMR-8115978. We also thank J. Provost for his assistance with some of the computer programming.

Registry No. $Fe(CN)_6^{4-}$, 13408-63-4; $Ru(CN)_6^{4-}$, 21029-33-4; $Os(CN)_6^{4-}$, 19356-45-7; $K_4Fe(CN)_6$, 13943-58-3; $K_3Co(CN)_6$, 13963-58-1; $K_3Rh(CN)_6$, 20792-40-9; $K_3Ir(CN)_6$, 20792-41-0.

(27) Hipps, K. W.; Knochenmuss, R. *J. Phys. Chem.* **1982**, *86*, 4477.
(28) Gauthier, S.; Klein, J.; Leger, A.; de Cheveigne, S.; Guinet, C. *J. Electron Spectrosc. Relat. Phenom.* **1983**, *30*, 209.
(29) Yang, W.; White, H. W. *Surf. Sci.* **1982**, *118*, 303.
(30) Dubois, L. H.; Hansma, P. K.; Somorjai, G. A. *Appl. Surf. Sci.* **1980**, *6*, 173.
(31) Kroeker, R. M.; Kaska, W. C.; Hansma, P. K. *J. Catal.* **1979**, *57*, 2.
(32) Hipps, K. W.; Mazur, U. *Rev. Sci. Instrum.* **1984**, *55*, 1120.
(33) Kirtley, J. R.; Hansma, P. K. *Phys. Rev. B: Solid State* **1976**, *3*, 2910.